

# Theoretical Study of Solvation Effects on Chemical Reactions. A Combined Quantum Chemical/Monte Carlo Study of the Meyer-Schuster Reaction Mechanism in Water

O. Tapia,\* J. M. Lluch,<sup>†</sup> R. Cardenas, and J. Andres<sup>‡</sup>

Contribution from the Department of Chemistry and Molecular Biology, Swedish University of Agricultural Sciences, Uppsala Biomedical Center, Box 590, 751 24 Uppsala, Sweden.

Received March 30, 1988

**Abstract:** Monte Carlo (MC) and ab initio analytical gradient MO techniques are used to study solvent effects on a solvent-assisted reaction. The mechanism of the acid-catalyzed rearrangement of  $\alpha$ -acetylenic alcohol to  $\alpha,\beta$ -unsaturated carbonyl compounds is examined. A careful analysis of MC samples simulating hydration effects strongly suggests solvent caging to be the mechanism required to convert the in vacuo reactant and product of the rate-limiting step (RLS), which are unstable species (saddle points) on the energy hypersurface, into transient species able to play a mechanistic role. MC solvation of the transition structure of the RLS for the oxygen-protonated 3-methyl-but-1-yn-3-ol plus one water molecule (minimal solvated model, MSM-TS) is analyzed. Thereafter, passive and active solvent effects on a simplified model (methyl groups are replaced by hydrogen atoms) of the MSM-TS have been studied by adding another solvent water molecule at a Pulay 4-21G basis set level. The supermolecule results show that the MSM-TS and the ancillary water molecule produces a hilltop which better describes the molecular steps leading to the allenol form rather than to represent a solvated TS in the RLS. Mechanistically, the transition state for the RLS may be obtained from the solvated reactant by the jump of one solvent molecule toward its nucleophilic center. From the results of MC simulations, it is apparent that the unrelaxed solvation shell is less efficient in solvating the MSM-TS than the relaxed one. The relaxation of the solvation shell around the poorly solvated MSM-TS opens the channel to the final products, i.e., to  $\alpha,\beta$ -unsaturated carbonyl compounds.

The theoretical representation of solvent effects to study chemical rates and reaction mechanisms in condensed phases is an important and difficult problem in chemical physics. The solvent may act in a variety of ways which range from passive effects to active involvement along the reaction pathway, thereby leading to a change of the molecular mechanism. Several methods have been developed to calculate solvent effects on reactive systems. Significant progress has been achieved by applying statistical mechanics of non-equilibrium processes<sup>1-3</sup> to passive solvation effects. An empirically calibrated valence bond method has been developed and successfully applied to describe chemical reactions in liquid state and enzymes.<sup>4</sup> The self-consistent reaction field (SCRF) theory of solvent effects<sup>5</sup> that permits incorporation of passive and active effects into the electronic wave function of the model system has been used to study proton exchange processes and enzyme-catalyzed reactions.<sup>6</sup> The application of this latter method requires information on the structure of the reactant's surroundings which, for reactions in liquid environment, is not usually available. As a step prior to using the SCRF theory, Monte Carlo (MC) simulations of water solvation effects permits gathering valuable information. A number of systems ranging from simple solutes in water to solvent structure around biomacromolecules, e.g., nucleic acids and enzymes,<sup>7</sup> have been studied. Applications in the field of solvent effects on reacting species have been reported by Madura and Jorgensen<sup>8</sup> and by Tapia and Lluch.<sup>9</sup> There, combined quantum chemical and statistical mechanical procedures are used. The quantum chemistry is done at an ab initio Hartree-Fock self-consistent field molecular orbital level, while the statistical mechanics are implemented with the Metropolis et al. algorithm<sup>10</sup> and appropriate intermolecular potentials.<sup>11,12</sup> This combined approach is applied to study passive and active solvation effects in the "solvent-assisted" reaction mechanism describing the acid-catalyzed rearrangement of  $\alpha$ -acetylenic alcohols to  $\alpha,\beta$ -unsaturated carbonyl compounds (Meyer-Schuster reaction<sup>13,14</sup>).

The Meyer-Schuster reaction corresponds to an apparent 1,3-hydroxyl shift in  $\alpha$ -acetylenic secondary and tertiary alcohols. Theoretically, this system is of particular interest since the solvent

plays an active role in the mechanism. The reaction can be accomplished either in hyperacid nonaqueous media or in highly acid aqueous solution.<sup>13</sup> The difference in mechanisms is reflected in the molecular events describing the rate-limiting step (RLS). In nonaqueous media solvent effects have a passive nature.<sup>15-17</sup>

(1) (a) Hynes, J. T. In *The Theory of Reactions in Solution (Theory of Chemical Reactions Dynamics)*; Baer, M., Ed.; CRC Press: Vol. IV, 1986. (b) Northrup, S. H.; Hynes, J. T. *J. Chem. Phys.* **1980**, *73*, 2700. (c) Grote, R. F.; Hynes, J. T. *J. Chem. Phys.* **1980**, *73*, 2715. (d) Grote, R. F.; Hynes, J. T. *J. Chem. Phys.* **1981**, *74*, 4465. (e) Grote, R. F.; Hynes, J. T. *J. Chem. Phys.* **1981**, *75*, 2191.

(2) (a) Balk, M. V.; Brooks, C. L.; Adelman, S. A. *J. Chem. Phys.* **1983**, *79*, 804. (b) Adelman, S. A. *J. Chem. Phys.* **1980**, *73*, 3145.

(3) (a) Mangel, M. *J. Chem. Phys.* **1980**, *72*, 6606. (b) Marchesoni, F.; Grigolini, P. *J. Chem. Phys.* **1983**, *78*, 6287. (c) Knessl, C.; Mangel, M.; Matkowski, B. J.; Schuss, Z.; Tier, C. *J. Chem. Phys.* **1984**, *81*, 1285. (d) Straub, J. E.; Borbovec, M.; Berne, B. *J. Chem. Phys.* **1985**, *83*, 3172.

(4) (a) Warshel, A. *J. Phys. Chem.* **1979**, *83*, 1640. (b) Warshel, A.; Weiss, R. *J. Am. Chem. Soc.* **1980**, *102*, 6218. (c) Warshel, A. *J. Phys. Chem.* **1982**, *86*, 2218. (d) Warshel, A.; Hwang, J. K. *J. Chem. Phys.* **1986**, *84*, 4978.

(5) (a) Tapia, O. In *Molecular Interactions*; Ratajczak, H., Orville-Thomas, W. J., Eds.; Wiley: Chichester, England, 1982; Vol. 3, Chapter 2. (b) Angyan, J.; Allavena, M.; Picard, M.; Potier, A.; Tapia, O. *J. Chem. Phys.* **1982**, *77*, 4723.

(6) (a) Tapia, O.; Johannin, G. *J. Chem. Phys.* **1981**, *75*, 3624. (b) Sanhueza, J. E.; Tapia, O. *THEOCHEM* **1982**, *6*, 131. (c) Longo, E.; Stamatato, F. M. G.; Ferreira, R.; Tapia, O. *J. Theor. Biol.* **1985**, *112*, 783.

(7) (a) Clementi, E.; Corongiu, G. *Ann. N. Y. Acad. Sci.* **1981**, *367*, 83. (b) Clementi, E.; Corongiu, G. In *Biomolecular Stereodynamics*; Sarma, R., Ed.; Adenine Press: New York, 1981; p 209. (c) Formili, S. L.; Vercauteren, D. P.; Clementi, E. *J. Biomol. Struct. Dyn.* **1984**, *1*, 1281.

(8) (a) Madura, J. D.; Jorgensen, W. L. *J. Am. Chem. Soc.* **1986**, *108*, 2517. (b) Jorgensen, W. L.; Chandrasekhar, J.; Buckner, J. K.; Madura, J. D. *Ann. N. Y. Acad. Sci.* **1986**, *482*, 198.

(9) Tapia, O.; Lluch, J. M. *J. Chem. Phys.* **1985**, *83*, 3970.

(10) Metropolis, N.; Rosenbluth, A. W.; Rosenbluth, M. N.; Teller, A.; Teller, E. *J. Chem. Phys.* **1953**, *21*, 1087.

(11) (a) Jorgensen, W. L. *J. Phys. Chem.* **1983**, *87*, 5304. (b) Jorgensen, W. L. *J. Am. Chem. Soc.* **1981**, *103*, 677. (c) Chandrasekhar, J.; Jorgensen, W. L. *J. Chem. Phys.* **1982**, *77*, 5073. (d) Jorgensen, W. L.; Madura, J. D. *J. Am. Chem. Soc.* **1983**, *105*, 1407. (e) Jorgensen, W. L. *J. Chem. Phys.* **1982**, *77*, 5757.

(12) Matsuoka, O.; Clementi, E.; Yoshimine, Y. *J. Chem. Phys.* **1976**, *64*, 1351.

(13) Swaminathan, S.; Narayan, K. V. *Chem. Rev.* **1971**, *71*, 429.

(14) Edens, M.; Boerner, D.; Chase, C. R.; Nass, D.; Schiavelli, M. D. *J. Org. Chem.* **1977**, *42*, 3403.

(15) (a) Andres, J.; Silla, E.; Tapia, O. *J. Mol. Struct. THEOCHEM.* **1986**, *138*, 171. (b) Andres, J.; Silla, E.; Tapia, O. *J. Mol. Struct.* **1983**, *105*, 307.

\* Permanent address: Department of Chemistry, Autonomous University of Barcelona, Bellaterra, Barcelona, Spain.

<sup>†</sup> Permanent address: Department of Physical Chemistry, Col.legi Universitari Castello, Valencia University, Spain.

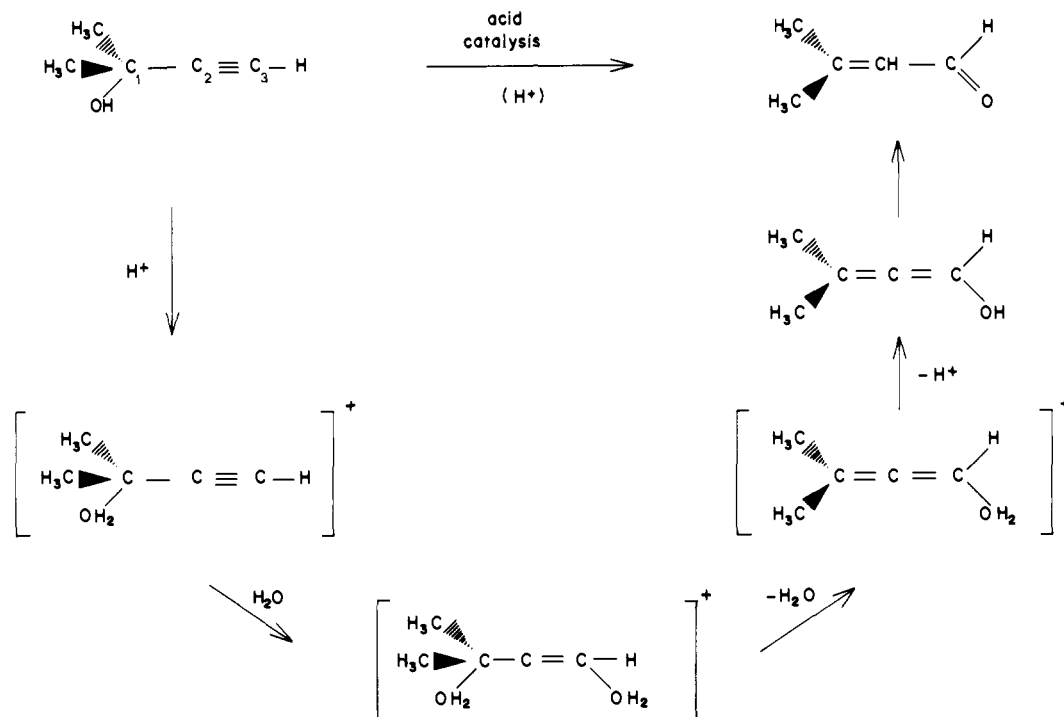


**Figure 1.** Schematic representation of the reaction mechanism proposed for aqueous acid solutions for the Meyer–Schuster reaction. The rate-limiting step involves the protonated species only.

In acid aqueous media, kinetic and isotopic substitution data<sup>14</sup> indicate a change in the molecular mechanism with active involvement of solvent water, the alkynyl C<sub>3</sub>-center (cf. Figure 1) undergoes a nucleophilic attack by a water molecule. The molecular events can be represented now with the protonated alcohol plus an ancillary water molecule: the minimal solvated model (MSM). Recently,<sup>17</sup> the 4-21G energy hypersurface for this reaction was characterized for the model system [(CH<sub>3</sub>)<sub>2</sub>C(OH<sub>2</sub>)C≡CH]<sup>+</sup> + H<sub>2</sub>O. Three geodesics<sup>17</sup> were found on the hypersurface: one reactive and two solvation geodesics (cf. Figure 2). This is the representation of the RLS; the corresponding saddle point describes the transition state (TS) proposed by Edens et al.<sup>14</sup> The two other geodesics describe solvation effects of the protonated alcohol and protonated allene, respectively. In the former case, the solvation sites are the —OH<sub>2</sub> group and the acetylenic carboacid ≡C—H (string SM1-R-SM2 in Figure 2); the solvation geodesic crosses the reactive one at the point corresponding to the reactant in the RLS. Along this solvation geodesic the reactant is a maximum, while along the reactive one it is a minimum. A similar situation is found in the allene region (string SM3-P-SM4 in Figure 2). One would expect that in vacuo the residence time at the “reactant” region to be short and probably of very little mechanistic value.<sup>18</sup> In water solvent, caging effects may be one way out of this situation. The question now is to establish whether or not manybody solvent effects can trap the saddle point into transient or metastable species to be mechanistically operational in Jenck’s sense.<sup>18</sup> To elucidate this aspect of solvent effects, detailed studies of Monte Carlo (MC) samples to get water distribution functions around chemically significant centers are carried out.

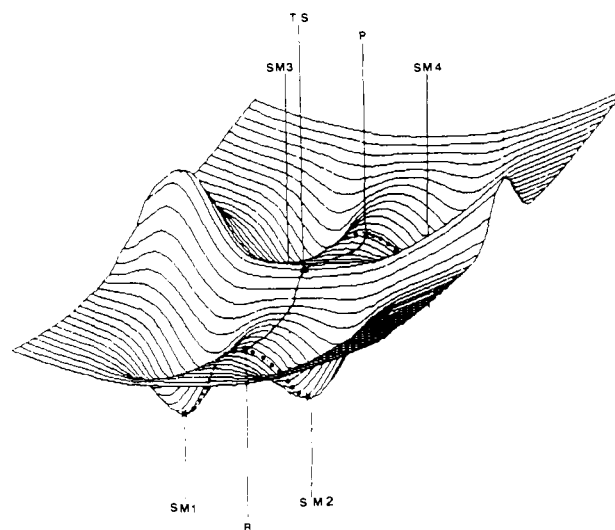


**Figure 2.** Schematic presentation of the energy hypersurface representing the solvation sites SM1 to SM4 and the reactant (R), product (P), and saddle point (TS) of the RLS.

The study of MC solvation of the MSM-TS in the RLS (string R-TS-P in Figure 2) has shown<sup>9</sup> the presence of water molecules around the alkynyl structure that were not in the MC solvation shell of the reactant. The MSM-TS is a fairly accurate portrait<sup>17</sup> of the transition structure derived from experimental information.<sup>14</sup> It is important, both from the mechanistical and methodological viewpoint, to determine the extent to which electronic and structural features of the MSM-TS are changed when solvation increases. This problem cannot be solved with MC methods alone, unless we have an adequate intermolecular potential function with an explicit dependence on intramolecular coordinates. Such a potential function is not easy to calculate at present. Instead, we focus attention on the effects an ancillary water molecule may have when it is included in the supermolecule approach: passive and active effects on the electronic structure of the MSM-TS are

(16) (a) Richey, H. G. Jr.; Rennick, L. E.; Kushner, A. S.; Richey, J. M.; Philips, J. C. *J. Am. Chem. Soc.* **1965**, *87*, 4017. (b) Richey, H. G.; Philips, J. C.; Rennick, L. E. *J. Am. Chem. Soc.* **1965**, *87*, 138. (c) Pittman, C. U.; Olah, G. A. *J. Am. Chem. Soc.* **1965**, *87*, 5632. (d) Olah, G. A.; Spear, R. S.; Westerman, P. W.; Denis, J. M. *J. Am. Chem. Soc.* **1974**, *96*, 5855.

(17) Andres, J.; Cardenas, R.; Silla, E.; Tapia, O. *J. Am. Chem. Soc.* **1988**, *110*, 666.

(18) Jencks, W. *Acc. Chem. Rev.* **1980**, *13*, 161.

studied. The initial ingoing water geometry is borrowed from MC information.

The quantum chemical evaluation of stationary points for the MSM plus ancillary water molecules require too many computing resources. For this reason the molecular model has been simplified by replacing the methyl groups of the initial model by two hydrogen atoms. At the same basis set level representation the stationary points for the methylated MSM and this simplified model are in full agreement. Passive solvation effects lead to a change in the hybridization degree at the nucleophilic center that contradict the evidence derived by Edens et al. The active solvation of the MSM-TS changes completely the structure of the MSM-TS; a study of a number of stationary points on the energy hypersurface (not reported here) strongly suggests such a structure is already a step forward in the molecular mechanism leading to the final  $\alpha,\beta$ -unsaturated carbonyl compound. Since the first stage in the molecular mechanism in liquid water must be a MC water in the solvation shell jumping to attack the C<sub>3</sub> center, one would expect the transition state of the RLS to be a poorly solvated MSM-TS structure. Thus, the geometry and electronic structure of the MSM-TS in solution would resemble the one calculated for the in vacuo model.

From this and related studies<sup>15,17</sup> two methodological conclusions follow. (i) The combined use of statistical mechanical simulation methods and quantum chemical supermolecule calculations is essential to get an adequate description of the mechanism in this water-assisted reaction. (ii) Supermolecule calculations alone with ancillary water molecules to represent solvation effects are not sufficient to establish the nature of the transition state structure for the reaction in solution. Neglect of manybody solvation effects is not warranted.

In section A of this paper we describe methods and models. Reaction mechanism and molecular models used in this work are presented in section B. Solvation effects as they are detected both in MC and quantum chemical calculations are presented and discussed in section C. An analysis of the present results contrasted to experimental information is given in section D. Conclusions are presented in section E.

## A. Methods

**I. Monte Carlo Simulations.** The MC simulations have been done by using Metropolis et al. algorithm.<sup>10</sup> The solute-solvent potential basically includes a solute shape term and the electrostatic interaction between effective atomic charges at the solute atoms and solvent dipole. Other details on the potential functions are given elsewhere.<sup>9</sup> The distribution functions for solvent oxygen and hydrogen atoms have been calculated over a sample of 600 K moves. These configurations were generated after equilibration of at least 1 000 000 configurations. To avoid correlations the sample is scanned by steps of 125. The origin of the distribution functions is put in turn on the C<sub>1</sub>, C<sub>2</sub>, and C<sub>3</sub> centers to sense the solvation shell in their respective neighborhood. For the TS sample the space has been divided into two hemispheres. The lower hemisphere contains the original protonated hydroxyl group and the water attacking C<sub>3</sub>.

The MC simulation of solvation effects were carried out with the geometries characteristic of the stationary points found in the R-TS-P string represented in Figure 2 with the methylated model. For the reactant, the ingoing water molecule which acts as a nucleophile on C<sub>3</sub> is about 3 Å from this center. At this distance there is no charge transfer from the protonated alcohol to this water molecule. For this reason the protonated alcohol frame in the reactant is surrounded by 125 water molecules. The initial configuration of MC water molecules is taken from an ice structure built up around the solute. The geometry of the remaining part of R was frozen. The solvation effects obtained are not biased by the specific quantum mechanical effects present in the MSM supermolecule. For the TS, the quantum mechanically determined geometry was frozen and solvated. The MC solvation reflects a solute system assumed to be in equilibrium with its surroundings. For the product the solvation study was done in a way similar to the reactant, mutatis mutandis.

**II. Quantum Chemical Procedure.** The procedure used to bracket stationary points<sup>17,19</sup> uses a partitioning of the internal coordinate space into two subspaces. One is the control space which includes all internal degrees of freedom, the force constant of which changes significantly as the reaction progresses. The complementary space is defined by the set

of internal coordinates that are subsidiarily changed as the reaction proceeds. The choice of these spaces is basically dictated by the mechanistic information available.<sup>17,19</sup>

The ab initio calculations have been performed with MONSTERGAUSS program.<sup>20,21</sup> The computations were carried out at split valence shell 4-21G<sup>22</sup> basis set level in the restricted Hartree-Fock formalism.<sup>23</sup> Analytic gradient<sup>24</sup> of the SCF HF energy with respect to the internal geometrical parameters have been used. Stationary points on the energy hypersurface have been located with the VA05 subroutine.<sup>25</sup> The hypersurface stationary point index has been determined by diagonalizing the symmetrized force constant matrix. The optimizations have been terminated after the gradient length of the unconstrained parameters (control space<sup>17,19</sup>) is reduced below  $5 \times 10^{-3}$  mdyne or mdyne Å/rad. The overall gradient length is somewhat better.

## B. Reaction Mechanism and Molecular Models

The reaction mechanism proposed for aqueous acid solutions is summarized in Figure 1. It comprises four steps. In the first, a rapid protonation takes place at the hydroxyl group. The second and rate-limiting step is an apparent 1,3-shift of the protonated hydroxyl group. The third step is presumably a rapid allenol deprotonation, followed by a keto-enol equilibrium that leads to the final product.

For nonaqueous media we have shown that the protonated alcohol leads to a transition-state structure that corresponds to an alkynyl cation interacting with a water molecule.<sup>15a</sup> The nonaqueous surroundings are most likely providing a passive solvation effect. The presence of alkynyl cations in this condition has been well documented experimentally.<sup>16</sup>

In aqueous acid solution we have used the intermolecular mechanism discussed by Edens et al.<sup>14</sup> as the basic model. As the discrete solvation increases by one water molecule the calculations with analytical gradients become extremely expensive. The methyl groups are therefore replaced by two hydrogen atoms, and the stationary points found in previous studies<sup>15,17,19</sup> are recalculated at Pulay 4-21G basis set level.

The simplified model presents the same hypersurface topography (cf. Figure 2): the stationary points describing R (protonated acetylenic alcohol) and P (protonated allenol) are themselves saddle points of order one on the global hypersurface.<sup>17</sup> The saddle points connect two solvation sites in the protonated alcohol (SM1 and SM2 in Figure 2) and protonated allenol (SM3 and SM4), respectively. It can be concluded that ab initio calculations of the MSM alone are not sufficient to give a complete theoretical background to Edens et al. mechanism. Solvent effects seem to be necessary to explain the mechanism. In vacuo, the lifetime of the reactant is bound to be too short to become a plausible species in the RLS mechanism.

## C. Solvation Effects

In liquid water one would expect that the hydroxyl and acetylenic C-H solvation sites might be occupied. The analysis of Monte Carlo solvation around C<sub>3</sub> is therefore of great mechanistic interest.

**I. Reactant Solvation at the MC Level.** In Figure 3 the water oxygen and hydrogen distribution functions around C<sub>3</sub> are presented. At 3.2 Å there is a very large peak in the oxygen atom distribution. Although the hydrogens may be in many cases pointing toward the C<sub>3</sub> center, there are water molecules correctly

(19) Tapia, O.; Andres, J. *Chem. Phys. Lett.* **1983**, *109*, 471.

(20) Peterson, M. R.; Poirier, R. A. Program MONSTERGAUSS, University of Toronto, Ontario, Canada 1980. In addition to the GAUSSIAN 70 integral and SCF routines, the program incorporates analytic gradients and automatic optimizations with or without constraints.

(21) Hehre, W. H.; Lathan, W. A.; Dichfield, R.; Newton, M. D.; Pople, J. A. GAUSSIAN 70 program, Q.C.P.E. No. 236.

(22) Pulay, P.; Fogarasi, G.; Pang, F.; Boggs, J. E. *J. Am. Chem. Soc.* **1979**, *101*, 2550.

(23) Roothaan, C. C. J. *Rev. Mod. Phys.* **1951**, *23*, 69.

(24) Schlegel, H. B. program FORCE, Ph. D. Thesis, Queen's University, Kingston, Ontario, Canada, 1975.

(25) Powell, M. J. D. VA05 program, Harwell Subroutine Library, Atomic Energy Research Establishment, Harwell, U.K.

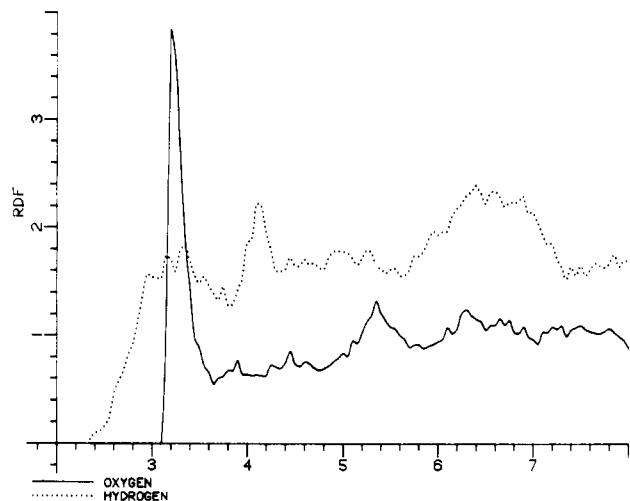


**Figure 3.** Water oxygen and hydrogen distribution functions around the  $C_3$  center for the protonated acetylenic alcohol.

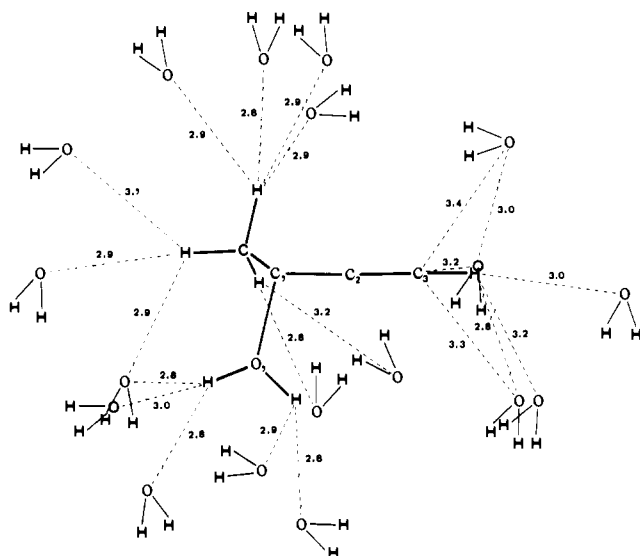


**Figure 4.** Schematic representation of one statistically significant solvation pattern around the protonated acetylenic alcohol (reactant) in the rate-limiting step. In the view one of the methyl groups hides the other. Distances are in Å.

oriented so as to initiate a nucleophilic attack onto  $C_3$ . The analysis of significant structures shows that the positions of these water molecules are basically determined by two facts: (1) the presence of a water molecule linearly H-bonded to the C-H acetylenic carboxic acid and (2) the existence of a set of water molecules H-bonded to the protonated hydroxyl group (cf. Figure 4).

In Figure 4a statistically significant solvation pattern of the reactant is depicted. The solvation sites at the C-H and the protonated alcohol are occupied by a number of solvent molecules. From the figure the presence of two water molecules able to produce a syn or an anti attack onto  $C_3$  is evident. Furthermore, the methyl groups bound to  $C_1$  have a well-defined set of H-bonded solvent water molecules. The relevance of the methyl group solvation pattern in connection with the related 1,2-hydroxyl shift reaction has already been discussed.<sup>9</sup> For the 1,3-hydroxyl shift reaction the remarkable fact is the presence of solvent water molecules occupying spatial positions apt to act as ingoing water molecules required by the MSM representation of the RLS.

The presence of water molecules that may play a reactive role in most interesting in view of the intrinsic properties of the energy hypersurface of the MSM. If the in vacuo MSM were to develop its potentialities, then the water molecule would be more probably found at any one of the potential solvation sites but not at the position required by the molecular mechanism. In a MC simulation these sites appear to be filled by solvent water molecules.

Furthermore, the sample scanning shows that there are also water molecules correctly positioned to attack  $C_3$ . This result can be described as a solvent caging effect if we look at it from the perspective of the in vacuo MSM hypersurface structure (cf. Figure 2). Thus, from the theoretical viewpoint, the reactant suggested by Edens et al. becomes a solvent stabilized species. Furthermore, both syn and anti attacks of a water molecule are allowed since the statistical sample shows a distribution of water molecules at those positions.

**II. TS Solvation at the MC Level.** The analysis of the solvation shell around the TS structure (methylated model) is carried out by dividing the space into two hemispheres (centered at  $C_2$ ); in the upper hemisphere there are the methyl groups and the  $C_3$ -H bond, while the water fragments at  $O_1$  and  $O_2$  are in the lower hemisphere.  $O_1$  corresponds to the protonated hydroxyl oxygen;  $O_2$  stands for the oxygen of the incoming water. The distribution functions of water depicted in Figure 5 a, (parts b, and c) represent the full space, lower and upper hemispheres, respectively. They are calculated with the origin at  $C_2$ .

Within the range of 4 Å, in the total radial distribution (Figure 5a) there is one peak at about 3.4 Å for the oxygen atom distribution. The hydrogen atoms distribution starts at shorter  $C_2$ -H distances. This may indicate that there is a non-negligible amount of hydrogen atoms pointing toward the  $C_2$  center. The distribution of oxygen and hydrogen atoms in the lower hemisphere view from  $C_2$  displays peaks higher than those for the total starting at 3.2 Å. The hydrogens have a pattern similar to the total distribution. The oxygen distribution senses a cluster of well-defined water between 3.2 and 3.8 Å. Beyond 4 Å the distribution is not representative of the solvation at  $C_2$ . In Figure 5c it can be seen that there is a peak at 3.4 Å which is small relative to the one found in the lower hemisphere.

From Figures 5 a, (parts b, and c) it can easily be seen that the nearest water from the statistical sample is in the lower hemisphere in a neighborhood of the water fragments. This is quite reasonable as one expects H-bonding and electrostatic interactions between the solvent water molecules, and those included in the MSM will produce favorable statistical weights. As in our previous work, the sample is scanned to obtain information on significant structural patterns around the MSM.

To get more detailed information a representative configuration is depicted in Figure 6. Here the water molecules found around the TS at distances less than 3.5 Å are depicted. By using as origin the water oxygen atom which is situated at 3.2 Å from  $C_2$  and 3.5 Å from  $C_3$  and  $C_1$ , the MC sample is analyzed in order to get the number of configurations having one water molecule in a given neighborhood. This is done by taking spherical shells of radii varying between 0.1 and 1.1 Å around the new center. 41% of the total configurations scanned have a water molecule in a shell of 0.4 Å around the selected region. We consider this solvation effect as statistically significant.

From Figure 6 it can be seen that there is another water molecule in a neighborhood of the  $C_2$  center which hydrogens point toward the  $C_2$  atom. This water molecule is below the plane  $O_1$ - $C_1$ - $C_2$ - $C_3$ - $O_2$ . This plane will be referred to as the MSM plane.

**III. Product Solvation at the MC Level.** The solvation pattern for the protonated allenol is given by the distribution functions around the  $C_1$  center in Figure 7. The distribution shows very little structure. In average there is one water molecule at 3.5 Å from the  $C_1$  center, which corresponds to the product in Edens et al. model. In analogy to the reactant, there are two solvation sites (at least), SM3 and SM4 in Figure 2. One of them represents the protonated hydroxyl group, and a methyl C-H bond provides a second solvation site. Again, P is a maximum along the solvation geodesic in vacuo. In all these arrangements in vacuo, the water molecule is too far away from  $C_1$ . It is presumably the MC water molecule that could find out the way to get at a proper distance to onset the TS structure while the solvation shell of the reactant has not yet relaxed.

The point is that the product for the RLS of Eden et al. model can be thought of as the solvent-stabilized form.

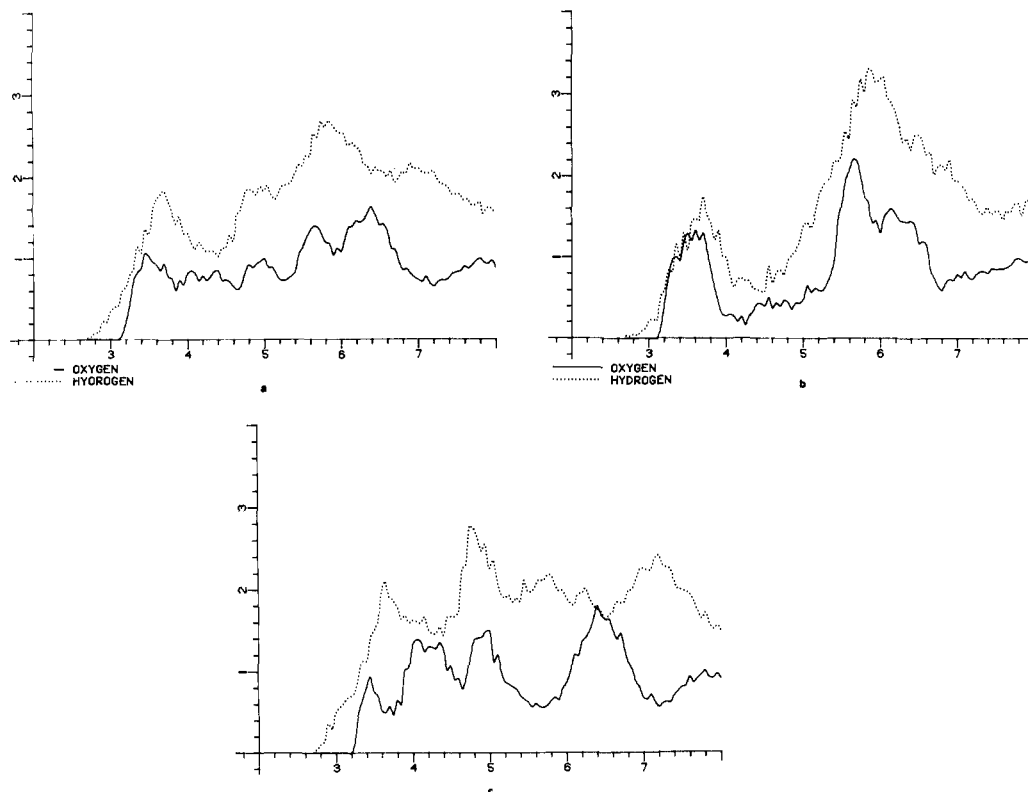


**Figure 5.** Distribution functions of water oxygen and hydrogen around the C<sub>2</sub> center in the transition structure characterizing the rate-limiting step. Figure 5a depicts the total distribution; 5b and 5c represent distribution functions calculated for the lower and upper hemispheres. The lower hemisphere contains the water fragments, and the upper one has the methyl groups.

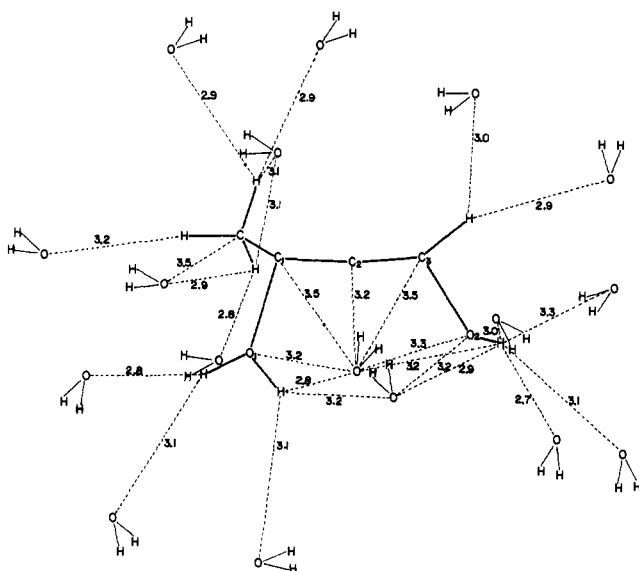


**Figure 6.** Schematic representation of one statistically significant solvation pattern around the transition structure in the rate-limiting step. In the view one of the methyl groups hides the other.

**IV. TS Solvation at the Supermolecule Level.** The solvation pattern of the MSM-TS structure found by MC simulations shows two solvent molecules in a neighborhood of C<sub>2</sub>. This situation raises a question on the robustness of the MSM-TS structure when water is explicitly considered at the quantum chemical level. The goal is to use quantum chemistry to study the effect of water molecules (in statistically significant positions, as determined by MC simulations) on the saddle point structure. This study is necessary since in previous quantum chemical calculations the TS structure in anhydrous medium differs from the MSM-TS structure. This latter contains one water molecule in addition to the anhydrous model; this new water plays a central role in determining the nature of the TS structure. The current study will

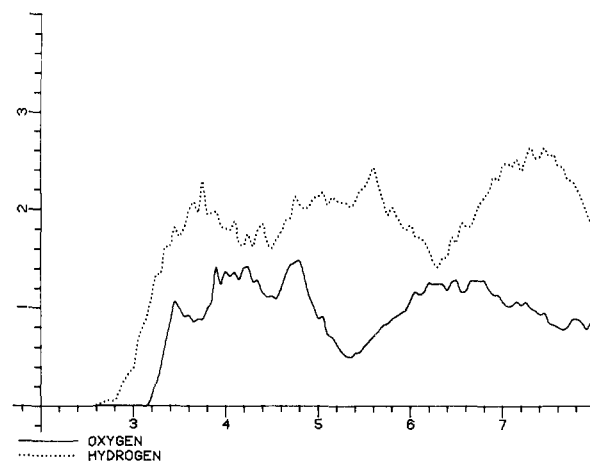


**Figure 7.** Oxygen and hydrogen distribution functions around the C<sub>1</sub> center for the protonated allenol (product) in the RLS.

involve quantum chemical calculations of the simplified MSM with one additional water molecule (MSM + H<sub>2</sub>O). Both, passive and active solvation models are considered. In the passive model, water enters in the supermolecule, but its internal geometrical parameters are not optimized. Basically, the water perturbs the active space of the MSM-TS. In the active solvation model, the intra and intermolecular degrees of freedom are included along with the MSM parameters into the active space; full geometry optimization is carried out.

**(a) Passive Solvation.** Supermolecule calculations with a solvent water molecule set up at the position found in the MC study (MC water) and the MSM structure frozen have been carried out in order to sense energy and force field changes. The starting point being the structure where the intermolecular distance between the MC water oxygen and C<sub>2</sub> makes an angle of 10° with respect to the normal vector to the MSM plane. Then, the water is moved down to 40° and then to 75°, and SCF calculations are carried out without any geometry optimization. The energy descends in

Table I.<sup>a</sup>

$\epsilon$	TS <sup>2</sup>		water frozen TS	
	-1.770	-0.052	-0.308	grad (Mdyne)
$\rho_{C_1C_2}$	0.051	0.104	0.123	-0.0099
$\rho_{C_2C_3}$	-0.039	0.008	-0.075	-0.0163
$\rho_{C_3O_2}$	0.254	0.032	0.614	-0.0028
$\rho_{O_2H_1}$	-0.092	-0.005	-0.018	-0.0150
$\rho_{C_1O_1}$	-0.211	-0.376	-0.501	-0.0106
$\rho_{O_1H_2}$	0.073	0.001	0.013	0.0109
$\rho_{C_2O_3}$	-0.017	-0.039	-0.0007	-0.0007
$\rho_{O_3H_3}$	-0.002	-0.001	0.0001	0.0001
$\rho_{C_2H_4}$	-0.068	-0.097	-0.0879	-0.0879
$\angle C_1C_2C_3$	-0.163	-0.433	-0.095	0.0112
$\angle H_3C_3C_2$	0.117	0.099	0.480	-0.0024
$\angle O_2C_3C_2$	0.093	-0.064	-0.080	-0.0099
$\angle H_1O_2C_3$	0.111	-0.010	0.059	0.0132
$\angle O_1C_1C_2$	-0.227	-0.070	-0.081	0.0008
$\angle H_2O_1C_1$	-0.108	-0.098	-0.139	-0.0263
$\angle O_3C_2C_1$	-0.839	0.310	-0.1274	-0.1274
$\angle H_3O_3C_2$	-0.014	-0.398	0.0361	0.0361
$\angle H_4C_2C_1$	0.138	0.324	0.1733	0.1733
$\tau_{H_6,7C_1C_2C_3}$	-0.056	-0.180	-0.275	0.0000
$\tau_{O_3C_2C_1C_3}$	-0.016	-0.217	-0.1013	-0.1013
$\tau_{H_3O_3C_2C_1}$	0.133	-0.022	-0.0053	-0.0053
$\tau_{H_4C_2C_1C_3}$	0.006	-0.425	-0.0579	-0.0579

<sup>a</sup>Negative eigenvalues ( $\epsilon$ ) and eigenvectors from the force constant matrix defined in the control space of 22 internal coordinates for the TS<sup>2</sup> (saddle point of order two). Passive solvation of an ancillary water and the MSM contains 13 parameters only; only one negative eigenvalue is found here; the gradients associated with each of the 22 internal coordinates for the passive solvation are indicated (grad).

1 kcal/mol when the angle changes from 10° to 40°. Even at 75° there is little gain in energy. The forces between the atoms inside the MSM structure are marginally affected by the MC water. Still, these points are not stationary.

Now, the control space of the MSM is reintroduced, and the degrees of freedom of the ancillary water are frozen. The reason for this constraint is easy to see: there are solvation sites, one at each ingoing and outgoing water fragment in the MSM structure, and one would expect a negative curvature in the angle variable connecting both points. The index of this point on the energy hypersurface of the MSM + H<sub>2</sub>O is one. The gradients of the full system indicate that the point is not stationary (cf. Table I water frozen TS). However, some useful information is obtained from this passive solvation if comparisons to the in vacuo MSM-TS are made: (1) The curvature of the variables included in the control space have not changed in nature. (2) The antisymmetric combination of C<sub>1</sub>-O<sub>1</sub> distance and C<sub>3</sub>-O<sub>2</sub> distance plus other important cross terms produce a negative curvature. (3) The relative weights in the reaction vector are fairly similar to the unsolvated MSM. (4) Passive solvation leave the MSM transition state topology invariant. (5) The geometry has, however, been changed; the complex has become more tightly bound (C<sub>1</sub>-O<sub>1</sub> and C<sub>3</sub>-O<sub>2</sub> distances are shortened). (6) The rehybridization at C<sub>3</sub> is more advanced than in the "in vacuo" MSM. (7) The charge transfer from the alkynyl structure toward O<sub>1</sub> and O<sub>2</sub> water fragments is somewhat increased (0.245 and 0.165, respectively). (8) The passive MC water does not gain positive charge (0.02) from the MSM-TS framework. (9) The C<sub>2</sub> center acts as a hydrogen bond acceptor as one would expect from the negative charge found in the in vacuo MSM-TS model.

The results summarized above reinforce some features found in the MC simulation, in particular, the presence of an H-bond between the MC water and the nucleophilic center C<sub>2</sub>. This point is of interest since the final product of this reaction ends up with a C-H bond at C<sub>2</sub>. However, from this and previous calculations it is foreseeable that the MC water may reorient itself and can also alter the geometric parameters of the MSM. It is, therefore, interesting to study the stationary point which is in the neighborhood of this point.

**(b) Active Solvation.** The SCF calculations are carried out with a control space containing all those variables characterizing the

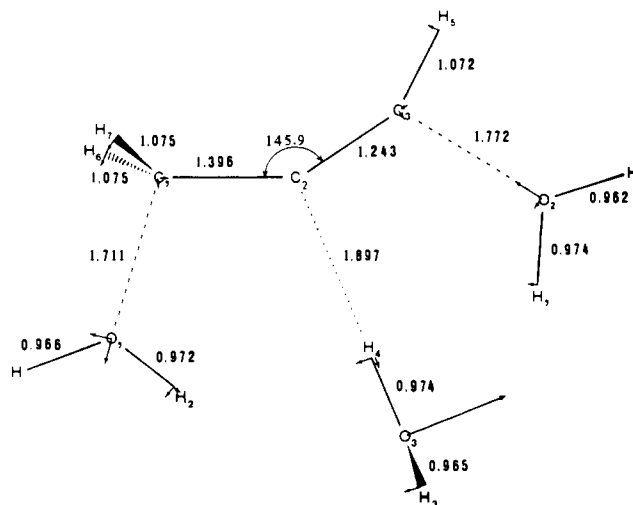


Figure 8. Geometry of the stationary point obtained from the MSM plus an ancillary water molecule. The diagonalization of the force constant matrix indicates that this is a saddle point of order two (TS<sup>2</sup>).

saddle point in the MSM plus the coordinates of the MC water. A stationary point is attained which has two negative eigenvalues. In Table I we report the information concerning the negative eigenvalues and corresponding eigenvectors obtained by diagonalizing the symmetrized force constant in the control space.

In Figure 8 the geometry of the stationary point is depicted. Structurally, some important facts emerge: (a) the nucleophilic center C<sub>2</sub> is now an H-bond acceptor which elicits the catalytic role played by the C<sub>2</sub> center;<sup>26</sup> (b) the active role of linear bending prompted by the electrophilic attack of water proton;<sup>27</sup> (c) tightening of C<sub>1</sub>-O<sub>1</sub> and C<sub>3</sub>-O<sub>2</sub> when compared to the passive solvated structure; (d) concomitantly, the rehybridization at C<sub>3</sub> has increased to become 50% of the product hybridization; (e) the incoming MC water (O<sub>3</sub>) is slightly out of the MSM plane.

In Figure 8 relative amplitudes of the eigenvector with eigenvalue -1.77 are shown with arrows. Displacement amplitudes along bonds and bond angles are depicted. For bendings, e.g.,  $\angle A-B-C$ , the displacement is represented as vectors perpendicular to the directions B-C and B-A. When the atom A or C is hydrogen, the displacement is assigned to H. The C<sub>2</sub> center displacement is arbitrarily frozen.

A displacement to the right in the direction of the vector with smallest eigenvalue (-1.77) brings the system to a minimum corresponding to the product in the MSM where the MC water molecule is solvating the protonated allenol. A displacement to the left leads to the solvated reactant in the MSM. The activation barrier on this new hypersurface is about 47 kcal/mol. This eigenvector is not exactly the one found in the MSM. The antisymmetric component in C<sub>1</sub>-O<sub>1</sub> and C<sub>3</sub>-O<sub>2</sub> is still there, but the dominating coefficient is the angular displacement of the ancillary water molecule.

Displacements following the eigenvector with eigenvalue -0.052 basically involve the MC water molecule and water fragment to the left (cf. Figure 8 and Table I) which are not related to the MSM mechanism. The interesting point is that the reorganization around the centers C<sub>1</sub> and C<sub>3</sub> help introduce a water molecule in the neighborhood of C<sub>2</sub> that would bring to the mechanism involving C<sub>2</sub> protonation and to the final product of the reaction.

Energetically, the structure in Figure 8 is only 6.6 kcal/mol lower than the 10° passive solvated structure (PSS). The displacement from the PSS to Figure 8 is done with C<sub>1</sub>-O<sub>1</sub> and C<sub>3</sub>-O<sub>2</sub>

(26) (a) Ramakrishnan, V. T.; Narayan, K. V.; Swaminathan, S. *Chem. Ind.* **1967**, 2082. (b) Benn, W. *J. Org. Chem.* **1968**, *33*, 3113. (c) Schlosarsarczyk, H.; Sieber, W.; Hesse, M.; Hansen, H. J.; Schmid, H. *Helv. Chim. Acta* **1973**, *56*, 875. (d) Pauling, H.; Andrews, D. A.; Hindley, N. *Helv. Chim. Acta* **1976**, *59*, 1233.

(27) (a) Andres, J.; Silla, E.; Bertran, J.; Tapia, O. *J. Mol. Struct. THEOCHEM* **1984**, *107*, 211. (b) Andres, J.; Cardenas, R.; Tapia, O. *J. Chem. Soc., Perkin Trans. 2* **1985**, 363.

variables displacing in a symmetric mode (both become shorter). The MC water is about 2 Å away from the MSM plane, while in the active solvation model it is nearly in the plane. As the MC water descends, there is a change in the sign of the curvature associated with the  $\angle C_1-C_2-O_3$  bend. Such change is related to the  $\angle C_1-C_2-C_3$  bending which widens the distance between the water fragments at C<sub>1</sub> and C<sub>3</sub> thereby producing the space required to put the ancillary water in the MSM plane.

#### D. Mechanism: Theory and Experiment

The energy hypersurface of the MSM + H<sub>2</sub>O has been thoroughly explored. The analysis of this hypersurface will be presented in detail elsewhere. We quote some results of interest for the present discussion. A comparison of the optimized geometry of the quantum chemically calculated MSM + 1H<sub>2</sub>O to the initial MSM-TS + MC water (passive solvation) strongly suggests the former structure represents an advanced stage of the overall reaction, i.e., this geometry requires extensive solvent rearrangement. In so far as the MSM-TS structure is concerned, its solvation by one water molecule shows that the stationary points found have lower energies than the poorly solvated MSM-TS. Furthermore, the hypersurface topography contains a representation not only of the RLS but also of the final products of the overall reaction, in particular, C<sub>2</sub> protonation. The calculations indicate that the allenol deprotonation step does not necessarily precede the keto-enol exchange as suggested in Figure 1.

The experimental aspects of the Meyer-Schuster reaction as discussed by Edens et al.<sup>14</sup> require a particular TS structure. A portrait of that TS was obtained with the *in vacuo* MSM-TS.<sup>17</sup> The passive and active supermolecule calculations on the MSM with an ancillary water molecule show a significant change of the geometry and degree of hybridization at C<sub>3</sub> and a strong H-bonding of water to C<sub>2</sub>. Such changes are incompatible with Edens et al. conclusions.

The incompatibilities between quantum chemical supermolecule modeling of solvation effects and experimental information illustrate the difficulties of such approach to represent solvent effects. If we introduce the MC information in the discussion a more satisfactory picture can be obtained. The following scenario may be an adequate description for the mechanism of this reaction: (1) Notice first that manybody effects force one MC water molecule at the position demanded by the MSM-R of Edens et al.<sup>14</sup> (2) The RLS must be associated to the formation of the TS structure by the jumping of a solvent water molecule toward C<sub>3</sub>.

(3) The activation of the reactive mode is faster than solvent collective motions as a whole: no sizable solvent reorganization is expected at this stage. (4) As a result, the MSM-TS appears to be poorly solvated since no water molecules were found at a distance smaller than 4 Å from the C<sub>2</sub> center in the solvent surrounding the protonated acetylenic alcohol. This situation prevents the production of the initial reactant leading to protonation at C<sub>2</sub>. (5) Relaxation of the solvation shell around the poorly solvated TS leads to a lower energy point (e.g. Figure 6). (6) Besides, by relaxing the solvation shell, the system will evolve toward the products of the overall reaction in a cascade, once the solvent water molecules attack the C<sub>2</sub> center.

The transition state in the rate-limiting step in liquid water can be described by an imperfectly solvated MSM-TS structure. The analysis on the MSM-TS presented in our previous paper<sup>17</sup> applies without modifications.

#### E. Conclusion

Two conclusions of methodological value may be obtained from this study.

First, the calculation of solvent effects on chemical reaction pathways with adiabatic statistical mechanical methods<sup>8</sup> may not be useful if the solvent participates in an active manner during the reaction. In the present example, nonadiabatic solvation of the MSM-TS structure seems to be the key step in describing the rate-limiting step.

Second, the use of *ab initio* supermolecule calculations to study solvation effects of transition-state structures may be misleading if manybody solvent effects are not taken into account. Such types of calculations have recently been used to study reagent, activated complex, and product for ammonia addition to formaldehyde catalyzed by zero, one, or two molecules of water.<sup>28</sup> For the present case such a procedure is not fully warranted.

**Acknowledgment.** J. M. Lluch gratefully acknowledges partial financial support from the Department of Molecular Biology at Uppsala. J. Andres thanks the Conselleria Cultura, Educacio i Ciencia de la Generalitat Valenciana for a post doctoral fellowship (Curs 1986-1987). O. Tapia acknowledges the Swedish Research Council (NFR) for financial support.

**Registry No.** [(H<sub>3</sub>C)<sub>2</sub>(H<sub>2</sub>O)CC≡CH]<sup>+</sup>, 89257-42-1; (H<sub>3</sub>C)<sub>2</sub>(HO)C≡CH, 115-19-5.